Electronic Supplementary Material (ESI) for Journal of Materials Chemistry A.
This journal is © The Royal Society of Chemistry 2021

Tuning interfacial chemical interaction for high-performance perovskite solar cell with PEDOT:PSS as hole transporting layer

Fei Wu, Kangrong Yan, Haotian Wu, Benfang Niu, Zhixin Liu, Yaokai Li, Lijian Zuo,* and Hongzheng Chen*

State Key Laboratory of Silicon Materials, MOE Key Laboratory of Macromolecular Synthesis and Functionalization, Department of Polymer Science and Engineering, Zhejiang University, Hangzhou 310027, P.R. China.

*E-mail: hzchen@zju.edu.cn (H. Chen), zjuzlj@zju.edu.cn (Lijian Zuo).

— Experimental Section

— Experimental Data

Experimental Section

***Materials*:** Methyl-ammonium iodide (MAI, 99%) was ordered from MaterWin. PbI_2 (99%) and (6,6)-Phenyl-C61-butyric acid methyl ester ($PC_{61}BM$, 99.5%) were purchased from Xi'an Polymer Light Technology Corp. Bathocuproine (BCP, 99%) and N,N-dimethylformamide (DMF, 99%) were purchased from TCI. Poly(3,4-ethylenedioxythiophene):poly-(styrenesulfonate) (PEDOT:PSS) aqueous solution (Al 4083) was purchased from Baytron. Lithium citrate tribasic tetrahydrate (98%), sodium citrate (98%) and tripotassium citrate (98%) were purchased from Adamas-beta. All reagents and solvents were used directly if not specified.

***Device fabrication*:** The ITO-etched glass substrates were cleaned sequentially in detergent (2%vol Hellmenex), deionized water, acetone, isopropanol and ethanol ultrasonic bath for 20 min, respectively. After then, the substrates were dried in air oven at the temperature of 100 ℃ and treated by UV-Ozone treatment for 20 min before using. The hole transporting layers were prepared by spin coating precursor solution on ITO glass and annealed at 120 ℃ for 20 min, the PC M-PEDOT HTL was obtained by doping Potassium citrate (PC) at different concentrations. The x PC M-PEDOT denotes the doping concentration (x) with a unit of mol/L. MAI and PbI_2 (1:1 mole ratio) were dissolved in N, N'-dimethyl formamide (DMF) with the concentration of 1.6 M. The spin-coating process was 4000 rpm and accelerated speed of 2000 rpm/s for 30 s, and started initially after dropping 30 μl perovskite precursor solution to the substrate, and

then 180 μl chlorobenzene (CB) was dropped at around 6 s, and 30 μl $PC_{61}BM$ (15 mg/ml in CB) solution was dropped at the following 15 s. After the spin-coating process, the perovskite layer was annealed at 100 ℃ for 5 min, and treated by DMF solvent vapor annealing (SVA) for 2 min. BCP (1 mg/ml in ethanol) was spin-coated at 3000 rpm for 30 s, followed by deposited 100 nm Ag in vacuum chamber under high vacuum of $2x10^{-4}$ Pa. The device area is 4 mm^2, which is defined by the shade mask.

***Characterization*:** The photocurrent density-voltage (*J-V*) measurement was performed via the solar simulator (SS-F5-3A, Enlitech) along with AM 1.5G spectra whose intensity was calibrated by the certified standard silicon solar cell (SRC-2020, Enlitech) at 100 mV cm^{-2}. The external quantum efficiency (EQE) data were obtained by using the solar-cell spectral-response measurement system (QER, Enlitech). The dark *J–V* curve was measured by Keithley source 4200. Film morphologies were studied through the scanning electron-microscope (SEM) images obtained from a Hitachi S-4800. The SEM images of the perovskite were attained by selectively removing the $PC_{61}BM$ layer from the perovskite/$PC_{61}BM$ film by rinsing with chlorobenzene (CB). The X-ray diffraction (XRD) patterns were recorded at a scan rate of 10° min^{-1} on Rigaku Ultima IV X-ray diffractometer with Cu Kα radiation (0.15406 nm). The steady-state photoluminescence (steady PL) was taken on an FLSP920 from Edinburgh Instruments.

Experimental Data

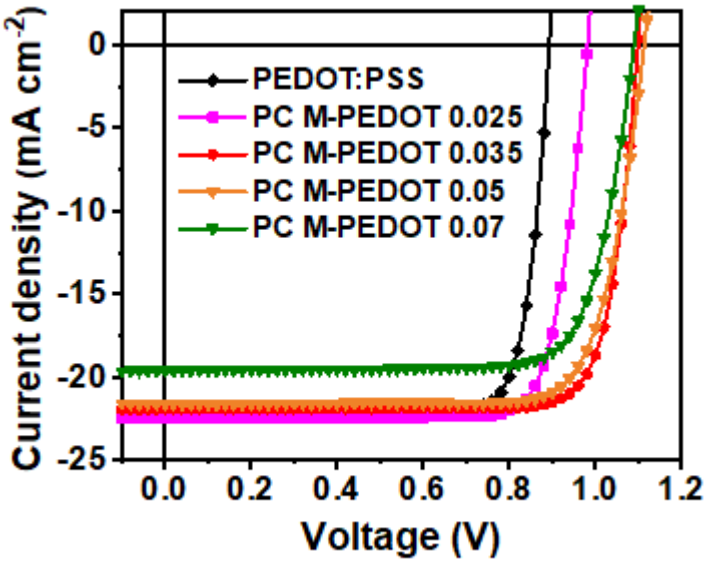

Fig. S1 *J–V* curves of sample performances with different concentrations of PC.

Table S1 Summary of sample performances with different concentrations of PC.

C (M)	V_{OC} (V)	J_{SC} (mA cm^{-2})	FF	PCE (%)
0	0.893	22.06	82.83	16.31
0.025	0.958	22.01	82.44	17.26
0.035	1.099	21.93	81.90	19.66
0.05	1.113	21.60	78.76	18.86
0.07	1.090	19.61	77.87	16.57

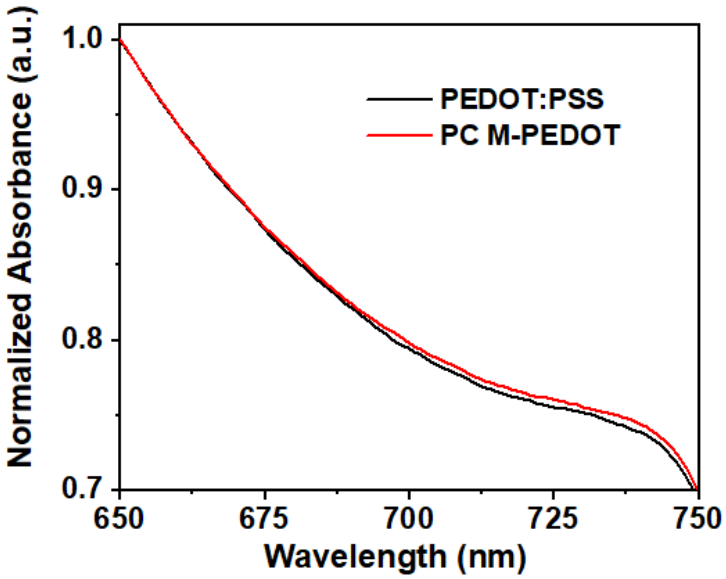

Fig. S2 Absorption spectra of $MAPbI_3$ perovskite films on ITO/PEDOT:PSS and ITO/PC M-PEDOT substrates.

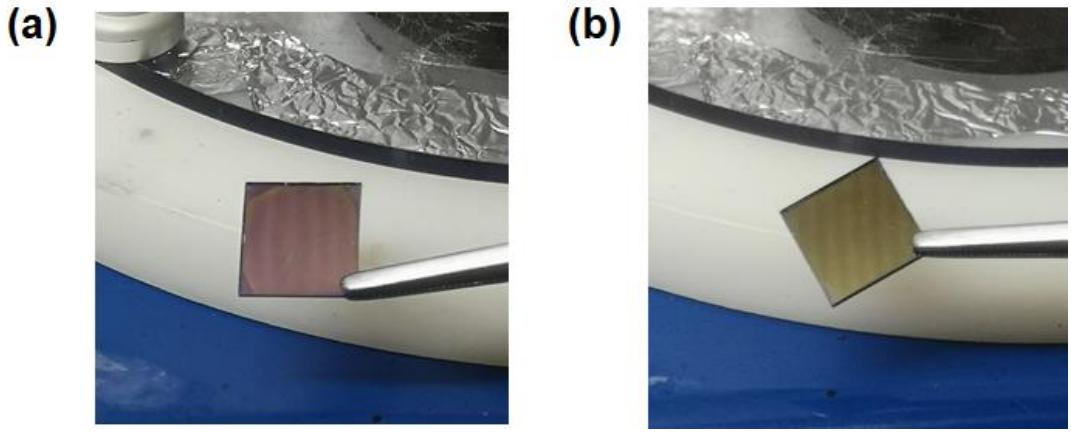

Fig. S3 Photos of the back of the ITO glass after spin-coating (a) PEDOT:PSS/$MAPbI_3$ and (b) PC M-PEDOT:PSS/$MAPbI_3$.

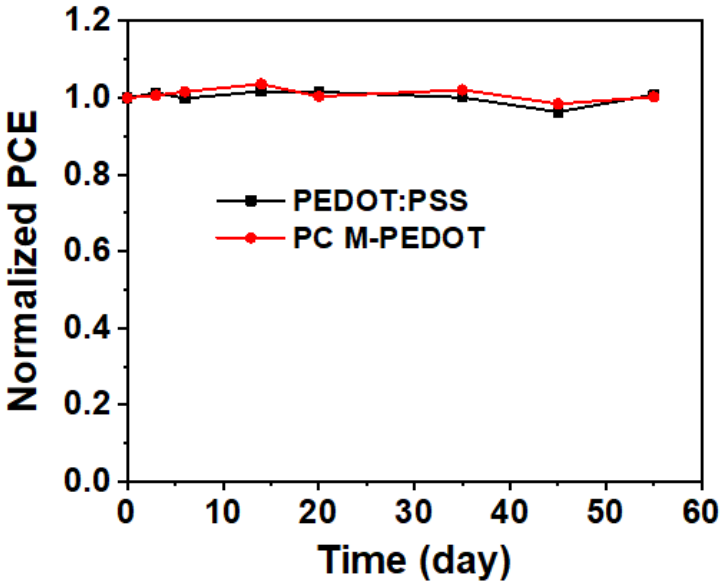

Fig. S4 The stability (in N_2) of PVSCs with different HTLs.

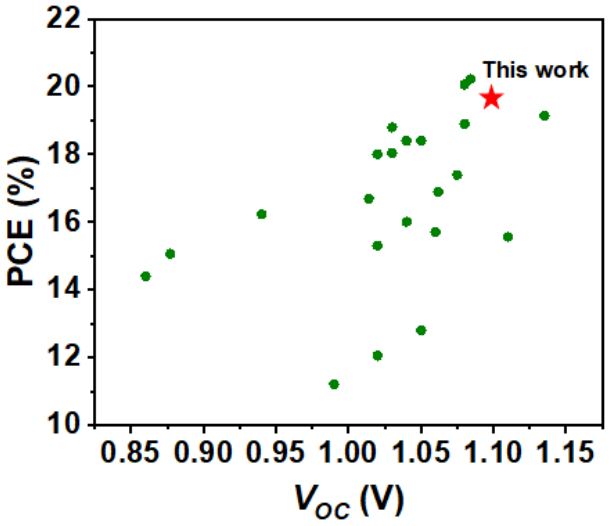

Fig. S5. The plot of PCE versus V_{OC} for the inverted PVSCs based on the PEDOT:PSS HTLs with doped, bilayer HTL and some other special treatments. (Details can be found in Table S2.)

Table S2 Summary of the performance for inverted $MAPbI_3$ PVSCs based on doped, bilayer HTL and special treatment of PEDOT:PSS HTLs. (ΔV_{OC} is the differential value of voltage boost device V_{OC} and reference V_{OC})

structure	V_{OC} (V)		ΔV_{OC}	Work Function (eV)		ΔWF	PCE (%)	year
	$^{a}V_{OC}$	$^{b}V_{OC}$		^{a}WF	^{b}WF			
ITO/PA-treated PEDOT:PSS/$MAPbI_3$/PCBM/Ag	0.842	0.877	0.035	5.2	4.8	-0.4	15.06	2015
ITO/m-PEDOT:PSS (1:2)/$MAPbI_3$/$PC_{61}BM$/Al	0.96	1.11	0.15	4.9	5.2	0.3	15.56	2016
ITO/b-PEDOT:PSS/$MAPbI_3$/$PC_{61}BM$/Bis-C_{60}/Ag	0.88	1.06	0.18	4.91	5.31	0.4	15.7	2016
ITO/GGO-PEDOT:PSS/$MAPbI_3$/$PC_{61}BM$/LiF/Al	0.93	1.05	0.12				12.8	2016
ITO/PEDOT:PSS/rub/$MAPbI_3$/$PC_{61}BM$/BCP/Ag	0.81	0.86	0.05	4.88	5.06	0.18	14.4	2017
ITO/PEDOT:PSS/BPQD/$MAPbI_3$/PCBM/Ag	0.915	1.014	0.099	5.1	5.2	0.1	16.69	2017
ITO/PDA:PEDOT:LS/$MAPbI_3$/PCBM/Al	0.86	1.02	0.16	5.0	5.45	0.45	12.05	2018
ITO/PEDOT:PSS/GO:PEG/MAPbI3/PCBM/Ag	0.962	1.062	0.1	4.9	5.2	0.3	16.89	2018
ITO/PEDOT:PSS/GO:PEG/$MAPbI_3$/PCBM/MoS_2/Ag	0.962	1.135	0.173	4.9	5.2	0.3	19.14	2018
ITO/PEDOT:PSS:NiPcS4/$MAPbI_3$/$PC_{61}BM$/BCP/Ag	1.02	1.08	0.06	5.08	5.14	0.06	18.9	2018
ITO/PEOz-PEDOT:PSS/$MAPbI_3$/$PC_{61}BM$/Bphen/Ag	0.96	1.075	0.115	4.9	5.3	0.4	17.39	2018
ITO/PEDOT:PSS-CsI/$MAPbI_3$/$PC_{61}BM$/Ag	1.003	1.084	0.081	5.10	5.26	0.16	20.22	2019
ITO/PEDOT:PSS:TX/$MAPbI_3$/C_{60}/BCP/Ag	0.90	0.94	0.04	5.30	4.88	-0.42	16.23	2019
ITO/PEDOT:PSS/SnO_2/$MAPbI_3$/$PC_{61}BM$/Ag	0.86	1.03	0.17	5.1	4.2	-0.9	18.04	2019
ITO/$Na_3C_6H_5O_7$-PEDOT:PSS/ $MAPbI_3$/$PC_{60}BM$/BPhen/Ag	0.92	0.99	0.07	5.11	5.06	-0.05	11.21	2019
ITO/urea-PEDOT:PSS/$MAPbI_3$/PCBM/Rhodamine/Ag	0.94	1.03	0.09				18.80	2019
ITO/PEDOT:PSS (EMIC)/$MAPbI_3$/$PC_{61}BM$/C_{60}/BCP/Ag	1.01	1.04	0.03				18.4	2019
ITO/PEDOT:PSS(EMIC)/$MAPbI_3$/S-acetylthiocholine chlorde /C_{60}/BCP/Ag	1.01	1.08	0.07				20.06	2019
ITO/PEDOT:PSS:CuSCN/$MAPbI_3$/PCBM/C_{60}/LiF/ Al	0.96	1.02	0.06				15.3	2020
FTO/PEDOT:PSS/NPB/$MAPbI_3$/$PC_{61}BM$/BCP/Ag	0.96	1.05	0.09	4.92	5.40	0.48	18.40	2020
ITO/PEDOT:PSS/SrGO/$MAPbI_3$/$PC_{61}BM$/BCP/Ag	0.99	1.04	0.05	5.02	5.34	0.32	16.01	2020
ITO/PEDOT:PSS-VOx/$MAPbI_3$/$PC_{61}BM$/C_{60}/Ag	0.84	1.02	0.18	5.0	5.5	0.5	18.0	2020
ITO/PC M-PEDOT/$MAPbI_3$/$PC_{61}BM$/BCP/Ag	0.893	1.099	0.206	4.89	4.55	-0.34	19.66	This work

$^{b}V_{OC}$ and $^{a}V_{OC}$ are the open-circuit potentials of PVSCs based on PEDOT:PSS with and without treatment, respectively. ^{b}WF and ^{a}WF are the work functions of PEDOT:PSS with and without treatment.

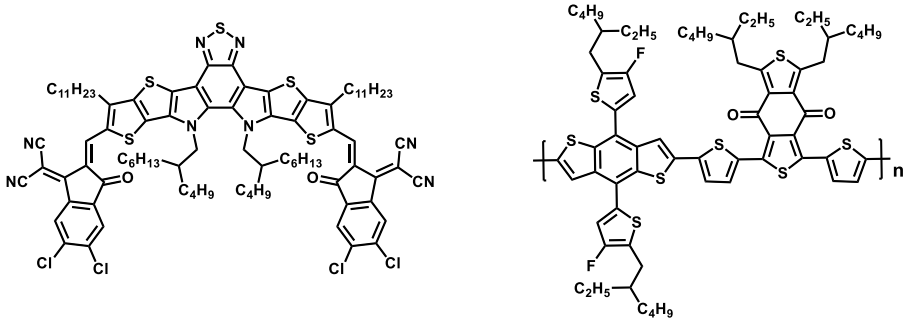

Fig. S6 The molecular structures of PM6 and BO-4Cl.

Table S3 Photovoltaic performances of PVSC and OSC with PEDOT:PSS and PC M-PEDOT under AM1.5 G illumination (100 mW cm^{-2}).

Device	HTL	V_{OC} (V)	J_{SC} (mA cm^{-2})	FF	PCE (%)
PVSC	PEDOT:PSS	0.916	19.17	77.19	13.55
($Cs_{0.05}MA_{0.09}FA_{0.81}Pb_1I_{2.86}Br_{0.09}$)	PC M-PEDOT	0.943	20.75	76.96	15.06
OSC	PEDOT:PSS	0.726	23.26	69.72	11.94
(PCE10:IEICO-4F)	PC M-PEDOT	0.590	23.45	44.24	6.20

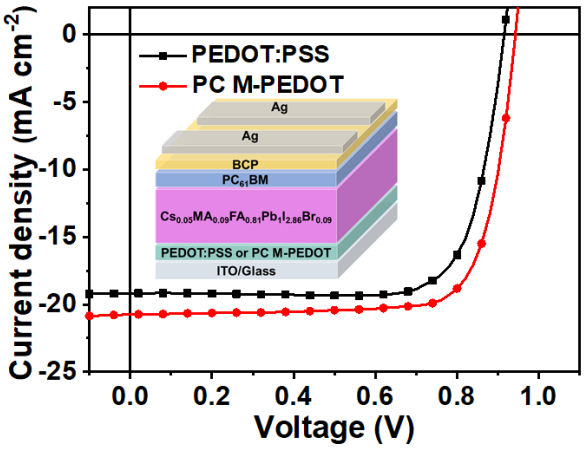

Fig. S7 The device performance of PVSCs with ITO/HTL/ $Cs_{0.05}MA_{0.09}FA_{0.81}Pb_1I_{2.86}Br_{0.09}$/$PC_{61}BM$/BCP/Ag configuration.

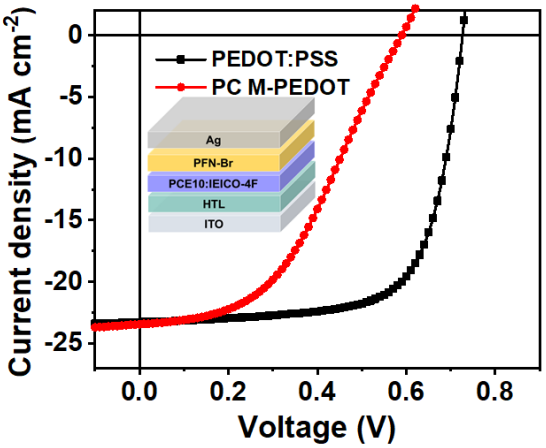

Fig. S8 The device performance of OSCs with ITO/HTL/PCE10:IEICO-4F/PFN-Br/Ag configuration.

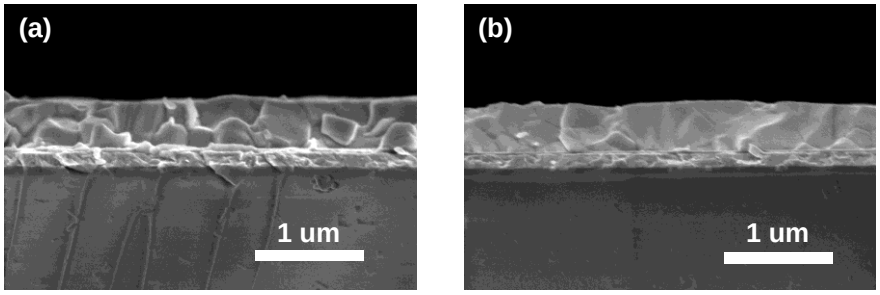

Fig. S9 Cross-sectional SEM images of perovskite films on (a) PEDOT:PSS and (b) PC M-PEDOT substrates.

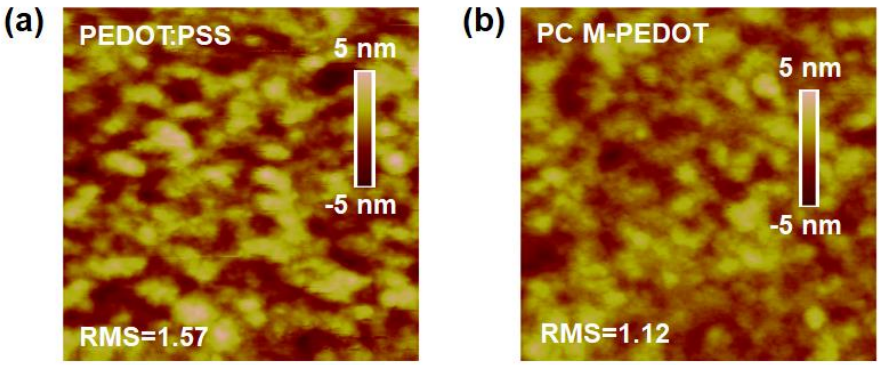

Fig. S10 AFM images obtained for the surfaces of (a) PEDOT:PSS and (b) PC M-PEDOT.

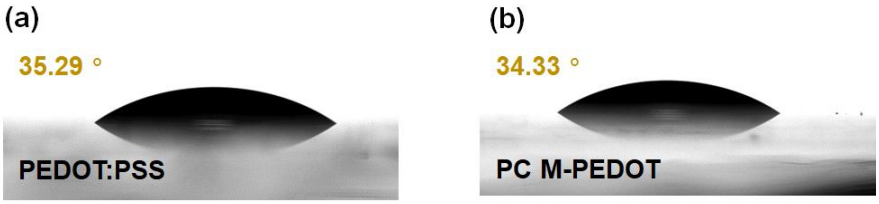

Fig. S11 Contact angles of (a) PEDOT:PSS and (b) PC M-PEDOT.

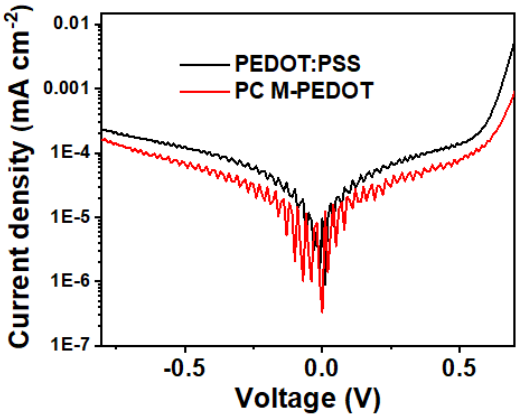

Fig. S12 J–V characteristics of PVSCs swept in the dark.

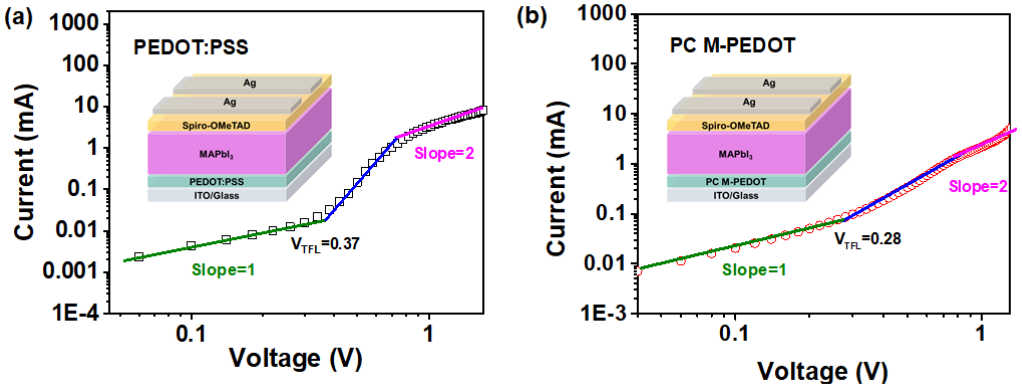

Fig. S13 *J–V* characteristics of devices with ITO/HTL/$MAPbI_3$/Spiro-OMeTAD/Ag configuration utilized for estimating the hole mobility and defect density for perovskite films on (a) PEDOT:PSS and (b) PC M-PEDOT.

Table S4 Photovoltaic performances of PVSCs with different HTLs under AM1.5 G illumination (100 mW cm^{-2}).

HTL	V_{OC} (V)	J_{SC} (mA cm^{-2})	$J_{SC}\,cal$ (mA cm^{-2})	FF	PCE (%)
PEDOT:PSS	0.893	22.06	20.96	82.83	16.31
0.035 CA	0.919	21.77	/	82.56	16.48
0.035*3 KAc	0.906	22.00	/	82.64	16.50
LC M-PEDOT	1.008	21.95	21.05	81.49	17.91
SC M-PEDOT	1.071	21.71	21.34	81.33	18.93
PC M-PEDOT	1.099	21.93	20.99	81.90	19.66